

 Open access • Journal Article • DOI:10.1016/J.TIFS.2019.02.001

A review on nuclear overhauser enhancement (NOE) and rotating-frame overhauser effect (ROE) NMR techniques in food science: Basic principles and applications

— [Source link](#) 

Ali Sedaghat Doost, Marzieh Akbari, Christian V. Stevens, Arima Diah Setiowati ...+1 more authors

Institutions: Ghent University, University of Isfahan

Published on: 01 Apr 2019 - Trends in Food Science and Technology (Elsevier)

Topics: Nuclear Overhauser effect and Two-dimensional nuclear magnetic resonance spectroscopy

Related papers:

- [Chapter 1: Application of the Nuclear Overhauser Effect to the Structural Elucidation of Natural Products](#)
- [New techniques in structural NMR — anisotropic interactions](#)
- [The nuclear Overhauser effect from a quantitative perspective.](#)
- [Chapter 8 – Correlations through space: The nuclear Overhauser effect](#)
- [Important 2D NMR Experiments](#)

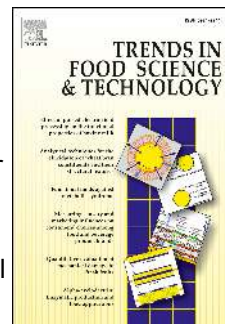
Share this paper:    

View more about this paper here: <https://typeset.io/papers/a-review-on-nuclear-overhauser-enhancement-noe-and-rotating-1dzyfqkn4u>

Accepted Manuscript

A review on nuclear Overhauser enhancement (NOE) and rotating-frame Overhauser effect (ROE) NMR techniques in food science: basic principles and applications

Ali Sedaghat Doost, Marzieh Akbari, Christian V. Stevens, Arima Diah Setiowati, Paul Van der Meeren



PII: S0924-2244(18)30674-5

DOI: <https://doi.org/10.1016/j.tifs.2019.02.001>

Reference: TIFS 2407

To appear in: *Trends in Food Science & Technology*

Received Date: 27 September 2018

Revised Date: 13 January 2019

Accepted Date: 1 February 2019

Please cite this article as: Doost, A.S., Akbari, M., Stevens, C.V., Setiowati, A.D., Van der Meeren, P., A review on nuclear Overhauser enhancement (NOE) and rotating-frame Overhauser effect (ROE) NMR techniques in food science: basic principles and applications, *Trends in Food Science & Technology*, <https://doi.org/10.1016/j.tifs.2019.02.001>.

This is a PDF file of an unedited manuscript that has been accepted for publication. As a service to our customers we are providing this early version of the manuscript. The manuscript will undergo copyediting, typesetting, and review of the resulting proof before it is published in its final form. Please note that during the production process errors may be discovered which could affect the content, and all legal disclaimers that apply to the journal pertain.

Background

The characterization of the original chemical structure and induced changes of micro- and macro-molecules using analytical techniques with concise and detailed outcomes is potentially one of the major challenges for food scientists. To this end, the non-invasive nuclear magnetic resonance (NMR) technique can play a significant role through employment of different NMR methods. The Nuclear Overhauser effect (NOE) and rotating-frame Overhauser effect (ROE) techniques are powerful NMR methods that have attracted great interest because they provide precise information about the three dimensional spatial structure of the molecules, as well as about possible chemical reactions and interactions.

Scope and approach

In this article, we reviewed the basic principles as well as applications of two NMR techniques: Nuclear Overhauser effect spectroscopy (NOESY) and rotating-frame Overhauser effect spectroscopy (ROESY). Hereby, we focused mainly on the applications and importance of these techniques in food science research. Both the structural (configuration and conformation) changes and the complexes formed by interacting compounds could be better studied using these techniques.

Key findings and conclusions

The inter- and intra-molecular interactions within food-based ingredient mixtures, as well as configurational and conformational analyses can be more efficiently studied with the aid of NOESY and ROESY. These methods as complementary analysis tools can be exploited for the straightforward elucidation of the spatial proximity of either novel, native or modified compounds. In the future, these techniques may be helpful to better understand the interaction between polymers, such as protein-polysaccharide interactions.

1 **A review on nuclear Overhauser enhancement (NOE) and rotating-frame Overhauser**
2 **effect (ROE) NMR techniques in food science: basic principles and applications**

3 *Ali Sedaghat Doost¹, Marzieh Akbari², Christian V. Stevens³, Arima Diah Setiowati¹, Paul Van der*
4 *Meeren¹*

5 ¹*Particle and Interfacial Technology Group (PalnT), Department of Green Chemistry and Technology,*
6 *Faculty of Bioscience Engineering, Ghent University, Coupure Links 653, Gent 9000, Belgium*

7 ²*Central Laboratory, Department of Analytical Chemistry, University of Isfahan, Isfahan, 81746-*
8 *73441, Iran*

9 ³*SynBioC Research Group, Department of Green Chemistry and Technology, Faculty of Bioscience*
10 *Engineering, Ghent University, Coupure Links 653, Gent 9000, Belgium*

11
12 **Background**

13 The characterization of the original chemical structure and induced changes of micro- and
14 macro-molecules using analytical techniques with concise and detailed outcomes is
15 potentially one of the major challenges for food scientists. To this end, the non-invasive
16 nuclear magnetic resonance (NMR) technique can play a significant role through
17 employment of different NMR methods. The Nuclear Overhauser effect (NOE) and rotating-
18 frame Overhauser effect (ROE) techniques are powerful NMR methods that have attracted
19 great interest because they provide precise information about the three dimensional
20 spatial structure of the molecules, as well as about possible chemical reactions and
21 interactions.

22 **Scope and approach**

23 In this article, we reviewed the basic principles as well as applications of two NMR
24 techniques: Nuclear Overhauser effect spectroscopy (NOESY) and rotating-frame
25 Overhauser effect spectroscopy (ROESY). Hereby, we focused mainly on the applications
26 and importance of these techniques in food science research. Both the structural
27 (configuration and conformation) changes and the complexes formed by interacting
28 compounds could be better studied using these techniques.

29 **Key findings and conclusions**

30 The inter- and intra-molecular interactions within food-based ingredient mixtures, as well
31 as configurational and conformational analyses can be more efficiently studied with the aid

32 of NOESY and ROESY. These methods as complementary analysis tools can be exploited for
33 the straightforward elucidation of the spatial proximity of either novel, native or modified
34 compounds. In the future, these techniques may be helpful to better understand the
35 interaction between polymers, such as protein-polysaccharide interactions.

36 **Keywords**

37 Nuclear magnetic resonance, Nuclear Overhauser enhancement, rotating-frame
38 Overhauser effect, stereochemical structure, complex inclusion

39 **1. Introduction**

40 The nuclear magnetic resonance technique, known as NMR spectroscopy, has been widely
41 utilized for more than 70 years. The early observation of NMR in solids and liquids goes
42 back to the 1940s when Isidor Rabi measured the magnetic properties of some nuclei
43 awarding the Nobel Prize. By now, the NMR technique is a frequently used analytical
44 method in basic and advanced research in different areas, mainly organic chemistry (Kumar
45 and Rani Grace, 2017). There are two types of NMR based on the resolution of the
46 obtained spectra: low and high resolution NMR. High resolution NMR spectra provide more
47 concise information about individual groups within one single molecule whereas these
48 individual contributions become unclear in low resolution NMR. For the first time, the
49 proton magnetic resonance spectrum was recorded at 30 MHz and explained by Arnold et
50 al. (1951) as a direct relation between the chemical shifts and the chemical structure of
51 ethanol. Since the 1950s, nuclear Overhauser enhancement (NOE) has become one of the
52 powerful and common tools in structural elucidation; the Overhauser effect of the nuclear
53 resonance in metallic lithium was initially observed through saturation of the electron spin
54 resonance (Vögeli, 2014, Carver and Slichter, 1953). The rotating-frame Overhauser effect
55 (ROE), which is basically similar to NOE, could be a potential alternative for NOE where the
56 NOE peaks become tremendously weak in the case of mid sized molecules with molecular
57 masses of about 1000 - 2000 Da. However, this phenomenon of decreasing NOEs is
58 dependent on the solution environment and the spectrometer frequency (Claridge, 2016b).

59 The rotating-frame Overhauser effect spectroscopy (ROESY) method was firstly proposed
60 by Bothner-By et al. (1984) to overcome the abovementioned problems. These two NMR
61 techniques are widely used not only in organic chemistry, but also in different research
62 areas and in particular in food science.

63 To the best of our knowledge, there is no review on the utilization of these techniques in

64 the field of food science. Therefore, the main focus of this review is firstly on the
65 fundamental theory of NOESY (nuclear Overhauser enhancement spectroscopy) and
66 ROESY, avoiding deep mathematical details because this is out of the scope of this review
67 paper. We attempted to shed light on these practical methods for food scientists in order
68 to gain a better understanding into the development of novel food products. Secondly, we
69 discussed the latest specific applications (in food science) of these two techniques in the
70 study of structural elucidation, conformational changes, and inclusion confirmation of
71 functional compounds. Finally, new insights in the current and prospective applications of
72 these techniques are provided.

73 **2. Theory**

74 **2.1. Nuclear Overhauser Effect (NOE)**

75 The nuclear Overhauser enhancement, also indicated as nuclear Overhauser effect,
76 concerns the net change of signal intensity from the enhanced spin (I) due to the relaxation
77 of a perturbed spin (S) that is dipole-dipole coupled to the first spin (Jung et al., 2000). In
78 other words, the cross relaxation of I due to dipole-dipole interaction either between
79 bonded nuclei or in the close vicinity of each other ($< 5 \text{ \AA}$) results in an alteration of the
80 spin population of I (Attaur et al., 2016, Claridge, 2016b, Kumar and Rani Grace, 2017,
81 Vögeli, 2014). Hereby, perturbation of spin S from its equilibrium population might
82 originate from saturation (equalizing the spin population differences) or inversion of a
83 resonance (inverting the population differences across the transitions). The result can be
84 visualized through a 2D-spectrum called nuclear Overhauser effect spectroscopy (NOESY).
85 There are additional cross peaks (arising from the NOE effect) besides many expected
86 NOESY diagonal peaks (corresponding to the 1D-spectrum peaks). Large molecules tend to
87 tumble more slowly (relax faster) in solution, which means that nuclear Overhauser effect
88 interactions need more time to be developed. On the other hand, small molecules tumble
89 more quickly in solution (relax slower); the movement of the nuclei allows a significant
90 development of dipolar interactions. The result is that NOESY cross peaks may be too weak
91 to be observed. Because the cross peaks in NOESY spectra emerge from spatial
92 interactions, this type of spectroscopy is particularly well suited to investigate
93 stereochemical relationships in a molecule. In fact, the aim of the NOESY NMR technique is
94 to identify spins undergoing cross-relaxation and also to measure the cross-relaxation
95 rates.

96 Typically, nuclei can have two types of magnetic interactions or couplings: dipole-dipole (D)
97 interaction (direct) and spin-spin interaction (indirect), which is known as scalar or J-
98 coupling. In terms of the NOE, the dipolar couplings that occur through space magnetic
99 interactions will be concerned (Claridge, 2016b).

100 Theoretically, NOE is defined as the variation of a resonance when the equilibrium of spin
101 populations is interfered with spin transitions of another. The magnitude of this transition
102 is stated as a relative intensity change according to the following equation (Gil and
103 Navarro-Vazquez, 2017):

104

105

Equation 1

$$N_I(S) = \frac{I - I_0}{I_0} \times 100 (\%)$$

106 where $N_I(S)$ shows the NOE of spin I once it has been perturbed by spin S, I is the intensity
107 in the presence of NOE, and I_0 is the equilibrium intensity. The enhancement is referred to
108 the intensity variation that can be potentially either negative or positive depending on the
109 motional characteristics (molecular size and solvent viscosity), sign of the spin's
110 gyromagnetic ratio, and the spectrometer frequency. Typically, NOE occurs when
111 longitudinal spin relaxation leads to the redistribution of the spin populations by transfer
112 from one nuclei spin population to the other resulting in perturbation. This would be as a
113 result of a stimulus i.e. the fluctuation of the magnetic field at the frequency relative to the
114 transition generated by molecular motion (Claridge, 2016b, Marco-Rius et al., 2014). The
115 rate of the relaxation is a function of the rotational correlation time (τ_c), an average time
116 needed for a molecule to rotate fully through an angle of 1 rad around any axis (Spyros and
117 Dais, 2012). Thus, molecules with a faster tumbling rate will have a short correlation time,
118 whereas slower tumbling molecules have accordingly a longer correlation time. Claridge
119 (2016a) suggested an approximate relation between the correlation time and molecular
120 weight (MW, in Da) as follows:

121

Equation 2

122

$$\tau_c \approx MW \times 10^{-12}(\text{s})$$

123 The power presented within a molecular motion leading to the transitions is called the
124 spectral density (Rule and Hitchens, 2006). For the transition mechanisms in the relaxation
125 processes, two possible relaxation processes (W_0 and W_2) can theoretically be

126 distinguished. The complete explanation of the energy states and spin transition is out of
127 the scope of this article and full details can be found in a book chapter by Gil and Navarro-
128 Vazquez (2017). The spectral density can exhibit useful information about how the
129 relaxation rates (W_0 and W_2) change against tumbling rates. Typically, a relatively higher
130 energy route (W_2) belongs to the molecules with the faster tumbling rate in a solution and
131 thereby demonstrate positive NOEs. On the other hand, slow tumbling rate molecules
132 promote the W_0 rather than W_2 leading to negative NOEs (Spyros and Dais, 2012). As the
133 relaxation rate (W) is inversely proportional to the internuclear separation distance (r^6), it
134 may cause a rapid reduction in NOE with increasing distance. Thus, the NOE can be most
135 likely observed when the distance between the protons is about 5 to 6 Å. Moreover, the
136 relaxation rate is directly dependent on the gyromagnetic ratio of the two spins. So,
137 variable rates might be obtained if the system is heteronuclear.

138 In the final 2-D NOE spectrum, there are two types of peaks known as diagonal and cross
139 peaks. Diagonal peaks indicate the proton peaks observed in the 1-D spectrum, whereas
140 the cross peaks indicate protons which are spatially close showing NOE interactions
141 between the correlated spins (< 5 Å) (Gil and Navarro-Vazquez, 2017, Claridge, 2016b). In
142 NOESY cross peaks, dipolar relaxation and exchange contributions cannot be distinguished
143 as both contribute and have the same sign.

144 Practically, NOESY measurements can be performed in two common forms (i.e. transient or
145 steady-state), known as two-dimensional NOESY and NOE difference techniques,
146 respectively. The former case is typically suitable for small ($MW < 1000$ Da) and large
147 molecules ($MW > 2000$ Da), in which the NOEs are positive and negative, respectively,
148 while the inversion of a target generates transient NOEs. On the other hand, NOE
149 difference can be applied for small molecules by generation of steady-state or equilibrium
150 NOEs from saturation of a target with positive NOEs (Claridge, 2016a, Kumosinski et al.,
151 1991).

152 Whereas steady-state NOE measurements are suitable for molecules that tumble rapidly in
153 a solution, larger molecules or small molecules in a viscous solution that tumble slowly can
154 be studied with the transient NOE technique. On the other hand, molecules with
155 intermediate molecular weight ($MW = 1000$ to 2000 Da) and tumbling rates between the
156 abovementioned conditions may have no or very weak NOE signals. Typically, NOESY is
157 used as a homonuclear ^1H technique. In this method, direct dipolar couplings provide the

158 primary means of cross-relaxation and spins undergoing cross-relaxation are those which
159 are close to each other in space. Thus, the cross peaks of a NOESY spectrum indicate that
160 protons are close to each other in space. For instance, those which rely on J-coupling to
161 provide spin-spin correlation and cross peaks, indicate that their protons are close to each
162 other e.g. by means of molecular bonds. The basic NOESY succession consists of three $\pi/2$
163 pulses. The first pulse creates transverse spin magnetization. This process happens during
164 the evolution time (t_1), which increments during the course of the 2D experiment. The
165 second pulse produces longitudinal magnetization that is equal to the transverse
166 magnetization component orthogonal to the pulse direction. Thus, the basic idea is to
167 produce an initial situation for mixing time (τ_m), the time elapsed when a target resonance
168 is monitored after initial inversion prior to the observation pulse and acquisition as a
169 function of exchange time (Canet, 2018, Claridge, 2016b, Gil and Navarro-Vazquez, 2017).
170 The third pulse creates transverse magnetization from the remaining longitudinal
171 magnetization. Acquisition immediately begins after the third pulse, and the transverse
172 magnetization is observed as a function of time (t_2). The NOESY spectrum is generated by
173 2D Fourier transform with respect to t_1 and t_2 . Axial peaks, which originate from
174 magnetization, have been relaxed during τ_m and can also be removed by an appropriate
175 phase cycling. NOESY spectra can be obtained in 2D absorption mode. Occasionally,
176 correlation spectroscopy-type artefacts appear in the NOESY spectrum. However, it is easy
177 to identify them by their anti-phase multiple structure (Winning et al., 2007).
178 NOESY suffers from a detrimental effect known as spin diffusion. Spin diffusion occurs
179 when other spins exist in close vicinity of the desired spins, which affect the magnetization
180 process leading to the creation of negative cross peaks (Poveda and Jimenez-Barbero,
181 1998). Rotating frame NOE techniques may offer an appropriate solution for this problem.

182 2.2. Rotating-frame nuclear Overhauser effect spectroscopy (ROESY)

183 Rotating frame nuclear Overhauser effect spectroscopy (ROESY) is similar to NOESY, but
184 the initial state is different. ROESY is sometimes called "cross relaxation appropriate for
185 minimolecules emulated by locked spins" (CAMELSPIN). Instead of observing cross
186 relaxation from an initial state of z-magnetization, the equilibrium magnetization is rotated
187 to the x-axis and then spin-locked by an external magnetic field, so it does not precess. This
188 method is useful for certain molecules of which their rotational correlation time is in the
189 range where the nuclear Overhauser effect is too weak to be detected, usually molecules

190 with a molecular weight around 1000-2000 Da. With respect to this range, several types of
191 molecules can be considered, including small molecule surfactants, glycosides, peptides,
192 macro-cyclic natural compounds, dimers of diterpenes, triterpenes, steroids, and large
193 alkaloids (Gil and Navarro-Vazquez, 2017).

194 In other words, ROESY and NOESY do not have a similar dependency on the correlation
195 time and the cross-relaxation rate constant. Therefore, a different τ_m should be set during
196 the pulse sequences (Chary and Govil, 2008). The pulse sequence of ROESY is basically
197 similar to the pulse sequence of homonuclear 2D experiments, which is a transverse
198 magnetization after a $\pi/2$ ^1H excitation followed by applying a spin lock period during τ_m
199 resulting in the detection of the proton resonances.

200 The selection of the appropriate mixing time for both NOESY and ROESY is critical. With a
201 short τ_m there would not be enough time for the NOE peaks to be observable or they are
202 weak. By contrast, at relatively longer times, the intensity peaks would be decayed through
203 relaxation. It should be taken into consideration that ROESY grows faster than NOESY and
204 therefore a shorter τ_m (300 - 400 ms) may be chosen (Gil and Navarro-Vazquez, 2017). The
205 readers are referred to Cavanagh et al. (2007) and Claridge (2016b) for the detailed
206 explanation about the experimental parameters and the choice of an optimum mixing time.

207 NOE intensities go from positive to negative as the correlation time increases, becoming
208 close to zero, whereas in ROESY the cross-relaxation rate constant is always positive (Figure
209 1). ROE and NOE have the same power for small molecules (around +38%). In terms of
210 larger molecules, NOE intensity values become bigger giving maximum intensity (negative
211 values), as compared to ROE. As can be seen in Figure 1, for medium size molecules, the
212 ROE is still positive and maximum, while the NOE goes theoretically to zero. Although these
213 values are not zero in practice, very small intensities will be recorded which makes the
214 interpretation impossible.

215 Unlike the NOESY cross peaks, dipolar relaxation peaks appear with a negative sign in the
216 ROE cross peaks, while the proton exchange peaks are positive, similar to the diagonal
217 peaks (Sandström and Kenne, 2006).

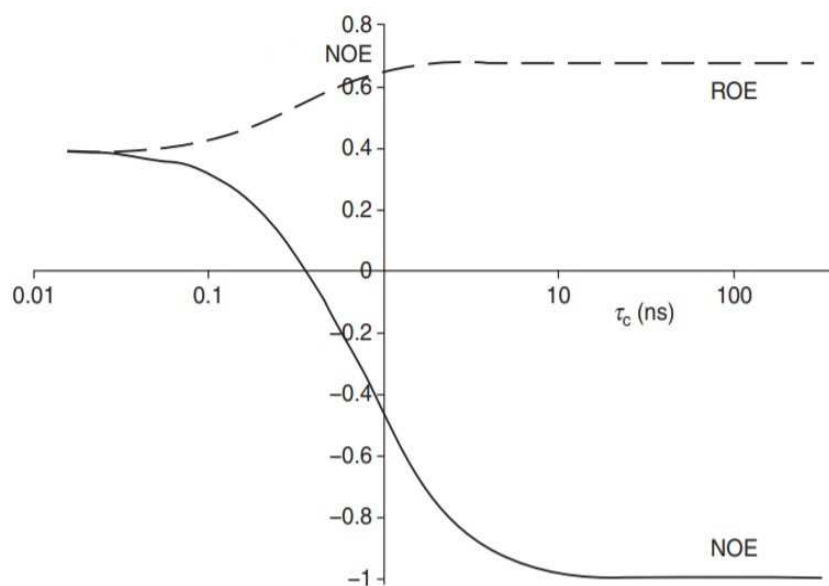


Figure 1. NOE (full line) and ROE (broken line) magnitudes as a function of molecular tumbling rate (τ_c), reprinted with permission from Williamson (2009).

218
219
220

221 Similar to other techniques, NOESY and ROESY also have some practical drawbacks that
222 should be considered. For instance, spin diffusion in large molecular weight molecules
223 (macromolecules) or lack of longitudinal cross relaxation can potentially interfere with the
224 NOE results (Allard et al., 1997). Although ROE suffers less from spin diffusion (direct ROE
225 cross peaks have opposite sign as three-spin effect cross peaks), homonuclear Hartman-
226 Hahn transfer of magnetization might be a problem for such quantitative studies. However,
227 off-resonance ROESY could be a solution (Allard et al., 1997).

228

229 3. NOESY and ROESY Applications

230 Typically, these techniques can be employed to study the spatial influence and relation
231 between nuclei of many compounds (Belloque and Ramos, 1999).

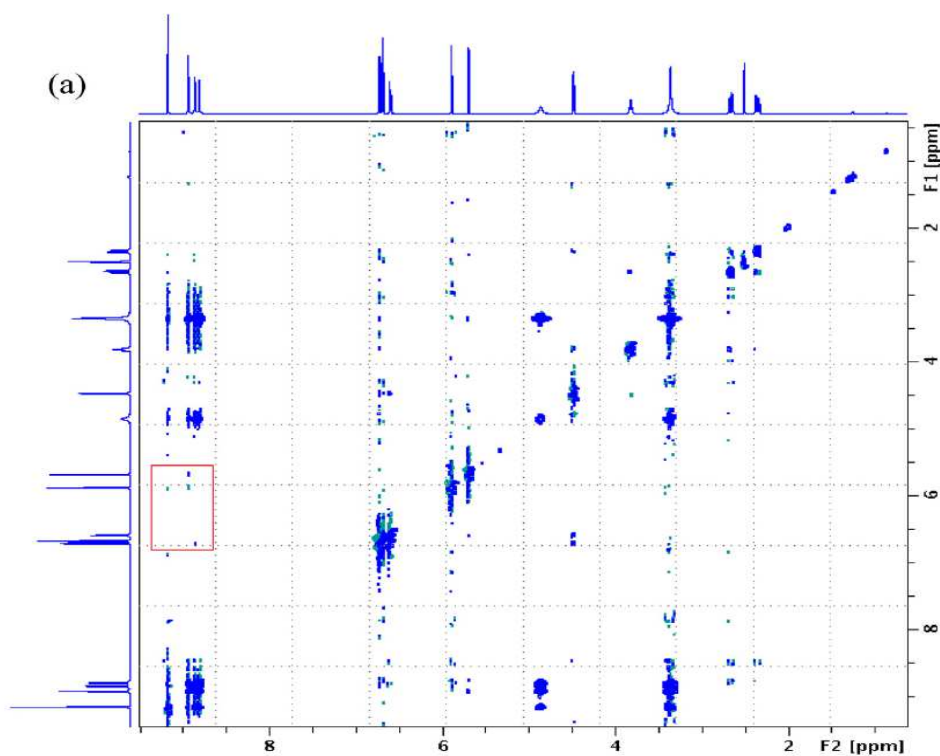
232 3.1. Structure elucidation

233 The structural characterization of organic compounds as well as of the secondary, tertiary,
234 or quaternary structure of biological micro- and macro-molecules can be identified using 1-
235 D or 2-D NOESY (Lau and Abdullah, 2017). For instance, NOESY is helpful to reveal the
236 nature of glycosylic linkages between sugar residues (Cui, 2005) or intra- and inter-residue
237 connectivity of molecules (Ai et al., 2016). Catechin polyphenol compounds are of
238 particular interest due to their contribution to health benefits, which is attributed to the
239 biological activity related to the hydroxyl groups in their chemical structure (Sedaghat
240 Doost et al., 2018c). Chemical shift fingerprinting of the substituted catechins was used to

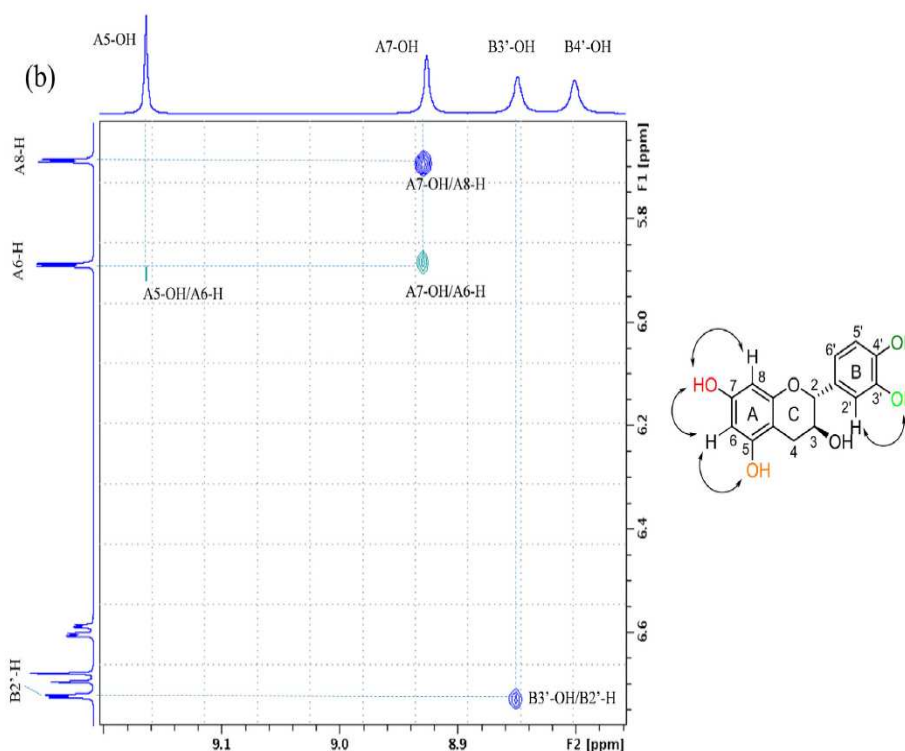
241 determine the structure profile of these compounds by Hong et al. (2017). The recorded
242 NOESY spectrum of the modified (+)-catechin hydrate is presented in Figure 2-a. The cross
243 peaks region of the protons within the hydroxyl groups is highlighted by a red square and
244 the enlarged view is shown in Figure 2-b. It can be seen that the $-OH$ group attached to C7
245 had a correlation associated with the protons of C6 and C8. Similarly, a cross peak was
246 observed, which shows the correlation of the hydroxyl hydrogen attached to C5 and the
247 proton connected to C6. The weaker contribution was attributed to the fact that there is
248 only one proton in the close vicinity of $-OH-C5$, which is H-C6, as can be seen from the
249 presented chemical structure in Figure2-b (Hong et al., 2017).

250

251



252



253

254 *Figure 2. The full (a) and enlarged (highlighted area by red rectangle in the full spectrum, b) NOESY spectrum of catechin.*255 *The NOESY correlation of the hydroxyl protons is also shown in the chemical structure (b). Reprinted from Hong et al.*256 *(2017) with permission from Elsevier.*

257 In a different study, the stereochemistry of goitrogenic 1,3-oxazolidine-2-thione
 258 derivatives, food compounds that may give (thyreo)toxicity to cruciferous vegetables, from
 259 Brassicales taxa was inferred by both NOESY and ROESY as complementary techniques to
 260 other NMR methods, as well as by selective homonuclear decoupling experiments
 261 (Radulović et al., 2017). Flavonoids are another group of food constituents which can
 262 chemically have an inter-flavonoid linkage that is susceptible to cleavage under different
 263 (e.g. acidic or alkaline) conditions. Different NMR techniques, including NOESY and ROESY
 264 can be employed to identify the inter-flavonoid interaction as well as the type of the upper
 265 and lower monomer units in order to recognize procyanidins from prodelphinidins (Teixeira
 266 et al., 2016, Esatbeyoglu et al., 2013).

267 In addition to the important role of the chemical structure of bioactive compounds for their
 268 absorption, their configuration is also believed to affect their bioavailability (Rein et al.,
 269 2013). For instance, it is shown that the S configuration of hesperitin-7-glucoside is more
 270 bioavailable than the R configuration (Lévêques et al., 2012). For a better understanding of
 271 the stereochemistry of such functional ingredients, NOESY and ROESY complementary
 272 techniques can be useful. For instance, twenty seven main bioactive compounds of *Ziziphus*

273 *jujuba* were isolated and their relative stereochemistry was established based on the
274 NOESY correlation peaks (Bai et al., 2016). Based on the NOESY spectrum analysis, either
275 *cis* or *trans* configurations were designated to the double bond present within the
276 structure of some studied compounds. Secondary metabolite terpene compounds such as
277 geranylphenol, mainly found in marine organisms, have been proved to be able to exert an
278 antifungal effect (Taborga et al., 2017). Recently, the chemical structure of some
279 geranylphenol compounds was evaluated by Taborga et al. (2017) who involved 1D NOESY
280 correlations in the chemical structure evaluation.

281 Since protobassic acid saponins present in *Sapotaceae* family plants are reported to have
282 cytotoxicity and antifungal properties, Chen et al. (2017) studied their isolation from the
283 kernels of *Palaquium formosanum*, which are thought to be effective as a prostate
284 anticancer. In this study, different analysis methods were used, including NMR techniques.
285 Together with those NMR techniques, NOESY spectrum interpretation revealed that there
286 was an equilibrium between two conformations of the 3' -deglycosylated 10 compound. In
287 fact, the determination of the structure of a new compound plays a key role to predict its
288 functional properties, which can be elaborated using NOESY or ROESY as complementary
289 techniques. To this end, Zeraik et al. (2016) conducted a comprehensive work to elucidate
290 the structure of a potential functional food ingredient from *Spondias tuberosa* fruit
291 combining various methods, including 2D NOESY.

292 A full list of recent articles published in food science related journals that used NOESY to
293 elucidate the chemical structure of food compounds is given in Table 1.

294 ROESY spectra were acquired by Masullo et al. (2017) with a 400 ms mixture time at 600
295 MHz to confirm the chemical structure of the extracted phenolic antioxidants from
296 hazelnut shells. It was evident from the intensity signals that there was a correlation
297 between the hydroxyl protons located in the same orientation, which ultimately resulted in
298 a final structure assignment together with other NMR analyses.

299 The exploration of new functional food sources has been a challenge to food scientists.
300 New lanostane-type bioactive compounds were found and characterized in the edible
301 portion of sea cucumbers by Elbandy et al. (2014). In their study, the relative
302 stereochemical structure of the isolated non-sulphated triterpene glycosides was
303 elaborated using ROESY with the aid of other NMR techniques. For instance, the α –
304 configuration of the oligosaccharide sequence and their attachment points were obtained

305 by interpretation of ROESY spectra. Iridoid monoterpenes, another type of functional
306 compounds, mainly found in Cornaceae family plants were isolated and identified with
307 different NMR techniques, including ROESY (Kucharska et al., 2015). The information about
308 the glycosilation position within the anthocyanin structure was thought to be worthwhile
309 for color stability assessment of maqui anthocyanins (Brauch et al., 2017). ROESY revealed
310 that the glucosyl moiety had a linkage to the delphinidin C-5 position in the studied
311 anthocyanin.

312

313

314

315

316

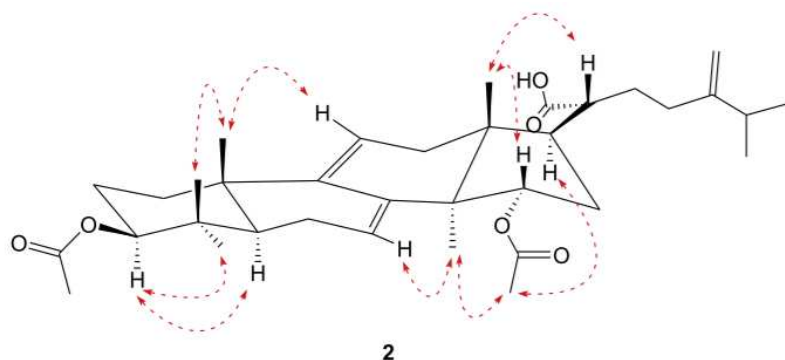
Table 1. Relevant examples of the structure elucidation of functional food ingredients based on NOESY.

Subject of the study	Reference
Arabinan-rich rhamnogalacturonan-I extracted from flaxseed	Ding et al. (2015)
Arabinoxylan purified and isolated from <i>Plantago asiatica</i> L. seeds	Yin et al. (2016)
Structural determination of catechin-(4-8)-dimer derivatives	Hayashi et al. (2018)
Non-starch polysaccharide extracted from roots of ginseng	Guo et al. (2015)
crude polysaccharide extracted from leaf skin of <i>Aloe barbadensis</i> <i>Miller (Aloe vera)</i>	Shi et al. (2017)
Prebiotic activity of mannanoligosaccharides isolated from palm kernel cake	Kalidas et al. (2017)
α -1, 6-linked galactomannan extracted from natural <i>Cordyceps sinensis</i>	Wang et al. (2017)
water-soluble heteropolysaccharide (TAPB1) purified from <i>Tremella aurantialba</i>	Du et al. (2015)
Isolation of a novel polysaccharide from <i>Boletus edulis</i>	Zhang et al. (2014a)
exopolysaccharides of <i>Lactobacillus casei</i> LC2W characterization	Ai et al. (2016)
A novel two-step enzymatic synthesis of Blastose	Miranda-Molina et al. (2017)
Neuroprotective sesquiterpenes isolated from <i>Petasites japonicus</i>	Wang et al. (2013)
α -Glucosidase inhibitor from <i>Buthus martensi</i> Karsch	Kim (2013)
Structure elucidation of <i>Baeckea frutescens</i> as an aromatic shrub	Jia et al. (2014)
New triterpene saponins from flowers of <i>Impatiens balsamina</i> L.	Li et al. (2017)
Isolation of a new caffeic acid derivative from <i>Tithonia diversifolia</i>	Pantoja Pulido et al. (2017)

317 3.2. Conformation and configuration analyses

318 NOESY and ROESY can be applied as complementary techniques to establish not only the
319 conformational changes of small and large molecules but also configurational variations
320 depending on the distances between nuclei, molecular motion speed, and the capability of
321 the functional groups in rotation (Efimov et al., 2016). The spectrum obtained from NOE
322 cross relaxation of the nuclear spins can be exploited to assign a conformation or
323 configuration. As the conformation of a chemical compound determines its unique
324 physical, chemical, and biological characteristics, it is substantial to distinguish the
325 conformation of a compound, particularly an unknown compound (Carey and Sundberg,
326 2007). Similarly, different configurations of a chemical compound may have a significant
327 influence on its physicochemical properties. For instance, the functional properties of a
328 polysaccharide (such as the nutritional, technological, and physiological features) vary
329 depending on the fact whether the polysaccharide has an α - or β -configuration (Hu et al.,
330 2017). The NOE spectrum as complementary data to 1-D ^1H and ^{13}C as well as
331 2D HMQC (Heteronuclear Multiple-Quantum Correlation) NMR spectra was interpreted to
332 determine the configuration of a glucan, an alkali-soluble polysaccharide extracted from an
333 edible mushroom (Hu et al., 2017). In another study, NOESY spectra combined with x-ray
334 diffraction data were used to establish the configuration of new cucurbitane-type
335 glycosides extracted from the fruits of *Momordica charantia* (Zhang et al., 2014b). Similarly,
336 the relative configuration of an ethanol extract of the sclerotia of *Poria cocos* was
337 determined using NMR and high resolution mass spectrometry analysis (Lee et al., 2017).
338 The relative configuration of some extracts was assigned by analysis of their NOESY
339 spectra, the coupling constants, and ^1H NMR chemical shifts. For instance, as the dashed
340 arrows display in Figure 3, a β -orientation was designated to compound 2 based on the
341 correlation between H-15 and H-18, as well as the correlation between an acetyl proton
342 with H-30 and H-17.

343



344

345 *Figure 3. NOESY proton correlations (dashed arrows) of compound 2 in the ethanol extract of the sclerotia of Poria cocos.*
346 *Reprinted from Lee et al. (2017) with permission from Elsevier.*

347 Carotenoids have different health benefits by decreasing the risk of diseases and among
348 them, allene carotenoids showed an anti-carcinogenic activity in mammals by triggering
349 apoptosis in certain tumor cell lines (Krinsky and Johnson, 2005, Agócs et al., 2018).
350 Recently, the relative configuration (axial and equatorial arrangements) of the isolated
351 allene carotenoids from mamey using acetone with subsequent saponification was
352 determined by the interpretation of the ROESY spectrum (Agócs et al., 2018). Previous
353 research has shown that specific functional foods can inhibit the degeneration of human
354 neurons leading to Alzheimer's disease. In a study performed by Xu et al. (2016), two new
355 functional sesquiterpenoids were isolated and different conformations as well as
356 configurations of an edible sesquiterpenoid were deduced using NOESY experiments.
357 Owing to the precise information obtained from the NOESY technique combined with 3D
358 modelling, a normal chair and envelope conformation was assigned to these
359 sesquiterpenoids.

360 A list of recent articles related to food compounds that used NOESY to determine the
361 structural conformation and configuration is given in Table 2.

362

363

364

365

366

367

368

369

Table 2. Overview of recent research to analyze the conformation and configuration of food components using NOESY.

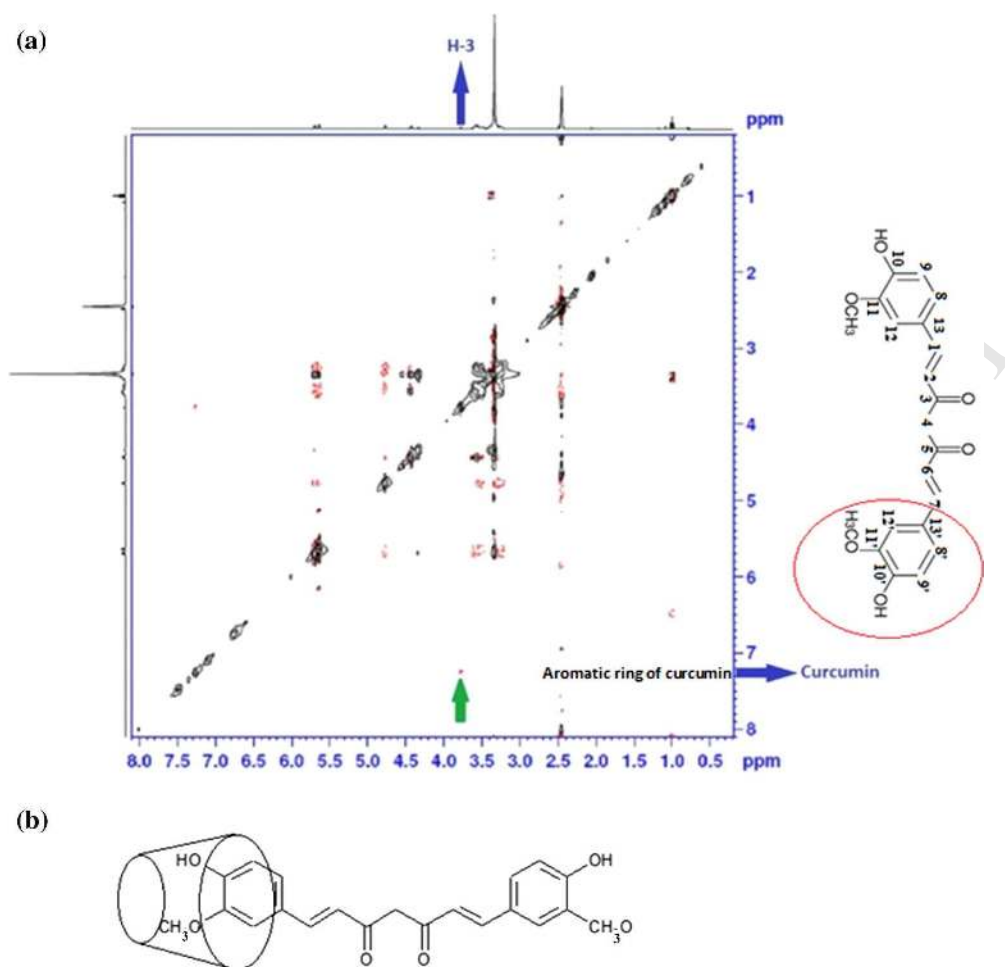
Subject of the study	Reference (year)
Sesquiterpenoids from <i>Petasites japonicus</i>	Xu et al. (2016)
Jasmonoid glucosides, sesquiterpenes and coumarins from the fruit of <i>Clausena lansium</i>	Xu et al. (2014)
Anti-inflammatory effect of <i>birsonimadiol</i> from seeds of <i>Byrsonima Crassifolia</i>	Pérez Gutiérrez (2016)
Sesquiterpene lactones and scopoletins from <i>Artemisia scoparia</i> Waldst. & Kit.	Cho et al. (2016)
Isolation and characterization of a polysaccharide from the fruiting bodies of <i>sanghuang</i> mushroom (<i>Phellinus Baumii</i> Pilát)	Ge et al. (2013)

370 3.3. Inclusion complexes

371 Another practical application of these techniques is to confirm the interaction of
372 compounds via complexation. They can be potentially employed as a direct proof for
373 spatial proximity between two molecules.

374 For instance, inclusion complexes of anethole (AN), a flavouring agent in bakery, sweets,
375 and alcoholic beverages, as a guest molecule within cyclodextrins (CD) as host molecules
376 were studied using 2D ROESY (Kfoury et al., 2014). In this work, they proved that anethole
377 penetrated the CD cavity via its ethylene group leading to the creation of complexes of the
378 AN aromatic ring in two different orientations within the CD cavity. Indeed, NOE cross
379 peaks indicated that AN molecules had an internal interaction with the CD cavity without
380 outside binding, which confirmed that AN was complexed inside the CD cavity. Likewise, in
381 another work, Jahed et al. (2014) showed that this technique was capable to confirm the
382 formation of complexes between the host and guest molecules; the complex of β -
383 cyclodextrin and curcumin was evaluated via NOE cross peaks (Figure 4) as well as by
384 changes in the chemical shift of internal protons. The results indicated that curcumin
385 formed a complex with β -cyclodextrin via its hydrophobic aromatic ring which promoted
386 the solubility of curcumin. This conclusion was derived from the presence of cross peaks
387 between the H-3 proton of β -CD and the protons from the aromatic ring of curcumin as
388 shown in Figure 4.

389



390
391 *Figure 4. Inclusion complex ROESY peaks (a) and schematic chemical structure (b) of curcumin incorporated within β -*
392 *cyclodextrin. Reprinted from Jahed, Zarrabi, Bordbar, & Hafezi (2014) with permission from Elsevier.*

393 The utilization of this technique could potentially provide us new insights in the functional
394 mechanism of host molecules. For instance, in the abovementioned work, one of the
395 proposed aims for encapsulation of curcumin within β -cyclodextrin was to enhance its
396 water solubility. Therefore, obtaining information about chemical and physical complexes
397 and knowledge about which part of the molecule is specifically involved in the interaction
398 of a guest molecule with other molecules may help to explore new delivery systems.

399 Recently, there has been a great demand for consumption of food products containing
400 natural ingredients, including essential oils (EOs). The latter are hydrophobic volatile
401 compounds that are increasingly attracting interest due to their antimicrobial and
402 antioxidant properties (Sedaghat Doost et al., 2018b, Sedaghat Doost et al., 2019).

403 Eugenol EO, primarily extracted from the flower buds of clove or cinnamon, was used in a
404 study by Gong et al. (2016) as a guest molecule inside the β -cyclodextrin host site. These
405 eugenol - β -CD complexes were intended to be used as an antifungal to preserve litchi
406 fruits during postharvest storage and transportation. In order to confirm the formation of

407 complexes and the interaction sites of the molecules, 2D NOESY spectra were acquired,
408 which revealed that eugenol interacted via the methyl group of its aromatic ring with the
409 lipophilic site inside the cavity. Similarly, carvacrol as a major constituent of some EOs
410 (Sedaghat Doost et al., 2018a, Sedaghat Doost et al., 2017) was encapsulated into β -CD not
411 only to promote its solubility but also to prolong the release and thereby enhancing its
412 functional features, such as its antimicrobial activity (Lavoine et al., 2014). This inclusion
413 was confirmed through 2D-NOE peaks. Lavoine et al. (2014) reported the dipolar
414 interaction between the aromatic group protons of carvacrol and the H-5 proton of β -CD in
415 its cavity.

416 CD, a biodegradable oligosaccharide, has been the subject of several studies owing to its
417 special chemical structure which enables it to make an inclusion complex with different
418 organic compounds. This increases their water solubility and therefore bioavailability
419 (Birck et al., 2016). Depth penetration of sodium benzoate, a preservative, inside the
420 hydroxypropyl- β -cyclodextrin cavity within a polyvinyl alcohol-citric acid film was
421 established using 2D ROESY. Birck et al. (2016) concluded from the proton correlations
422 obtained by ROESY cross peaks that sodium benzoate was successfully placed inside the
423 cavity and the Job's method analysis showed that the stoichiometry of the interaction
424 between hydroxypropyl- β -cyclodextrin and sodium benzoate was 1:1.

425 Another study carried out by Matencio et al. (2017) showed the host-guest inclusion
426 complex of oxyresveratrol, a stilbenoid extracted from mulberry fruits, with a modified CD
427 using NOESY. Similar to the previously mentioned studies, the analysis of the correlated
428 protons exhibited that the oxyresveratrol aromatic ring was involved in an interaction with
429 the internal cavity.

430 In another case, the interaction of caffeine with an aqueous solution of di-O-caffeoylquinic
431 acid was studied. In this research, analyses of NOESY and ROESY peaks revealed that the
432 three methyl groups of caffeine interacted with the aromatic groups of di-O-caffeoylquinic
433 acid isomers (D'Amelio et al., 2015).

434

435 **3.4. Other applications**

436 An alternative application is using NOESY as a tool for solvent suppression, primarily in
437 metabonomic studies. Most biological or medicinal samples have to be analyzed in water,
438 which makes the observation of relevant peaks challenging. Although in most of the cases

439 deuterated water (5-10 %) is added to do a lock spin, the prominent proton peak of water
440 prevents the efficient detection of solutes with low concentration (i.e. mM range)
441 (Claridge, 2016c, Kew et al., 2017). In order to suppress the proton peak of water (i.e.
442 reduce the magnitude of the solvent resonance) before it can be detected by the receiver,
443 several approaches have been suggested, including saturation, zero net excitation, and
444 destruction using pulsed field gradients of the water resonance (Cavanagh et al., 2007, Ross
445 et al., 2007).

446 The non-selective 1-D NOESY-based approach, which is obtained at short mixing times
447 (usually 0 to 10 ms), is commonly utilized in metabonomics for solvent suppression.
448 Recently, digested food samples were studied to figure out the amino acid fraction that is
449 solubilized at different digestion levels (Ménard et al., 2018). The final amino acid
450 composition of the digested proteins through the infant gastrointestinal tract was analyzed
451 using different techniques, to determine the extent of digestion. Solvent suppression was
452 applied using first increment NOESY NMR and the relative proton intensity of the
453 solubilized products of proteolysis was obtained.

454 The composition of the complex mixture of gut microbiota could be studied to establish
455 low molecular weight metabolites in fecal waters and study the relation between the host
456 metabolism and constituents of gut microbiota (Le Roy et al., 2015). To analyze these types
457 of samples using NMR, water suppression had to be applied. A presaturation approach
458 using NOESY was carried out prior to recording metabolic and fecal water spectra (Matysik
459 et al., 2016). It has been shown that the microbial activity during fermentation of dairy
460 products can be investigated using mass spectrometry or NMR techniques. The metabolites
461 of set-yoghurt containing different proteolytic strains of *Streptococcus thermophilus* co-
462 cultured with *Lactobacillus delbrueckii* subsp. *Bulgaricus* was studied using ^1H NMR
463 spectroscopy, but 1-D NOESY was utilized for solvent suppression (Settachaimongkon et al.,
464 2014). Dellarosa et al. (2016) also used a NOESY sequence to suppress the signal of residual
465 water in order to study the final metabolic profiling of fresh apples treated with pulsed
466 electric fields using high resolution ^1H NMR spectroscopy.

467

468 **4. Conclusions and future research**

469 The basic principles of two NMR techniques including nuclear Overhauser and rotating-
470 frame Overhauser effect and their applications in food science were thoroughly reviewed.

471 Whereas NOESY is mostly appropriate for relatively large and small molecules, ROESY could
472 be a more efficient choice for mid-sized molecules (1000-3000 Da). The chemical structure
473 of novel extracts or compounds could be elucidated using these methods. Moreover, the
474 conformation, configuration, as well as inclusion complex formation of chemical structures
475 can be determined using these NMR techniques in combination with other analysis tools.
476 Practically, only very low amounts of the sample (microliter) are needed, which provides a
477 big advantage because of the cost or the limited availability of specific samples. However,
478 NMR techniques are generally not considered as highly sensitive methods, and hence
479 require a relatively high concentration (preferably in the mM range). Moreover, in the
480 selection of the method and the practical parameters, some detrimental effects such as
481 spin diffusion should be taken into consideration.

482 In the future, these techniques can be potentially significant analysis tools for the
483 development of novel food products. The valuable information about the chemical
484 structure of food constituents obtained by these methods could substantially proceed the
485 production of innovative foods. For instance, protein and polysaccharide interaction has
486 been widely studied as it has a number of different applications, e.g. in food science.
487 Despite the complex chemical structure of proteins like whey protein isolate, which is a
488 mixture of different proteins, useful information of the interaction sites with
489 polysaccharides might be obtained through these techniques rather than present computer
490 simulations. The conformation and binding site of surfactants on the surface of oil droplets
491 as well as the effect of environmental conditions on their chemical structure may be
492 another future perspective that can be considered using NOESY and ROESY NMR methods
493 in food science.

494 **Acknowledgements**

495

496 **References**

- 497 AGÓCS, A., MURILLO, E., TURCSI, E., BÉNI, S., DARCSI, A., SZAPPANOS, Á., KURTÁN, T. & DELI, J.
498 2018. Isolation of allene carotenoids from mamey. *Journal of Food Composition and*
499 *Analysis*, 65, 1-5.
- 500 AI, L., GUO, Q., DING, H., GUO, B., CHEN, W. & CUI, S. W. 2016. Structure characterization of
501 exopolysaccharides from *Lactobacillus casei* LC2W from skim milk. *Food Hydrocolloids*, 56,
502 134-143.
- 503 ALLARD, P., HELGSTRAND, M. & HÄRD, T. 1997. A method for simulation of NOESY, ROESY, and Off-
504 Resonance ROESY spectra. *Journal of Magnetic Resonance*, 129, 19-29.
- 505 ARNOLD, J. T., DHARMATTI, S. S. & PACKARD, M. E. 1951. Chemical effects on nuclear induction
506 signals from organic compounds. *Journal of Chemical Physics*, 19, 507-507.
- 507 ATTAUR, R., CHOUDHARY, M. I. & ATIATUL, W. 2016. Chapter 6 - Nuclear Overhauser Effect. *Solving*
508 *Problems with NMR Spectroscopy (Second Edition)*. Boston: Academic Press.
- 509 BAI, L., ZHANG, H., LIU, Q., ZHAO, Y., CUI, X., GUO, S., ZHANG, L., HO, C.-T. & BAI, N. 2016. Chemical
510 characterization of the main bioactive constituents from fruits of *Ziziphus jujuba*. *Food &*
511 *Function*, 7, 2870-2877.
- 512 BELLOQUE, J. & RAMOS, M. 1999. Application of NMR spectroscopy to milk and dairy products.
513 *Trends in Food Science & Technology*, 10, 313-320.
- 514 BIRCK, C., DEGOUTIN, S., MATON, M., NEUT, C., BRIA, M., MOREAU, M., FRICOTEAUX, F., MIRI, V. &
515 BACQUET, M. 2016. Antimicrobial citric acid/poly(vinyl alcohol) crosslinked films: Effect of
516 cyclodextrin and sodium benzoate on the antimicrobial activity. *LWT - Food Science and*
517 *Technology*, 68, 27-35.
- 518 BOTHNER-BY, A. A., STEPHENS, R. L., LEE, J., WARREN, C. D. & JEANLOZ, R. W. 1984. Structure
519 determination of a tetrasaccharide: transient nuclear Overhauser effects in the rotating
520 frame. *Journal of the American Chemical Society*, 106, 811-813.
- 521 BRAUCH, J. E., REUTER, L., CONRAD, J., VOGEL, H., SCHWEIGGERT, R. M. & CARLE, R. 2017.
522 Characterization of anthocyanins in novel Chilean maqui berry clones by HPLC-DAD-
523 ESI/MSn and NMR-spectroscopy. *Journal of Food Composition and Analysis*, 58, 16-22.
- 524 CANET, D. 2018. Chapter 1 Introduction to Nuclear Spin Cross-relaxation and Cross-correlation
525 Phenomena in Liquids. *Cross-relaxation and Cross-correlation Parameters in NMR:*
526 *Molecular Approaches*. The Royal Society of Chemistry.
- 527 CAREY, F. A. & SUNDBERG, R. J. 2007. Stereochemistry, Conformation, and Stereoselectivity. *In:*
528 CAREY, F. A. & SUNDBERG, R. J. (eds.) *Advanced Organic Chemistry: Part A: Structure and*
529 *Mechanisms*. Boston, MA: Springer US.
- 530 CARVER, T. R. & SLICHTER, C. P. 1953. Polarization of nuclear spins in metals. *Physical Review*, 92,
531 212-213.
- 532 CAVANAGH, J., FAIRBROTHER, W. J., PALMER, A. G., RANCE, M. & SKELTON, N. J. 2007. CHAPTER 6 -
533 EXPERIMENTAL ¹H NMR METHODS. *In:* CAVANAGH, J., FAIRBROTHER, W. J., PALMER, A. G.,
534 RANCE, M. & SKELTON, N. J. (eds.) *Protein NMR Spectroscopy (Second Edition)*. Burlington:
535 Academic Press.
- 536 CHARY, K. V. R. & GOVIL, G. 2008. *NMR in Biological Systems*, Netherlands, Springer Netherlands.
- 537 CHEN, H.-Y., LIU, J.-F., TSAI, S.-F., LIN, Y.-L. & LEE, S.-S. 2017. Cytotoxic protobassic acid saponins
538 from the kernels of *Palaquium formosanum*. *Journal of Food and Drug Analysis*, 26, 557-
539 564.
- 540 CHO, J.-Y., JEONG, S.-J., LEE, H. L., PARK, K.-H., HWANG, D. Y., PARK, S.-Y., LEE, Y. G., MOON, J.-H. &
541 HAM, K.-S. 2016. Sesquiterpene lactones and scopoletins from *Artemisia scoparia* Waldst. &
542 Kit. and their angiotensin I-converting enzyme inhibitory activities. *Food Science and*
543 *Biotechnology*, 25, 1701-1708.
- 544 CLARIDGE, T. D. W. 2016a. Chapter 6 - Correlations Through the Chemical Bond I: Homonuclear
545 Shift Correlation. *High-Resolution NMR Techniques in Organic Chemistry (Third Edition)*.
546 Boston: Elsevier.

- 547 CLARIDGE, T. D. W. 2016b. Chapter 9 - Correlations Through Space: The Nuclear Overhauser Effect.
548 *High-Resolution NMR Techniques in Organic Chemistry (Third Edition)*. Boston: Elsevier.
- 549 CLARIDGE, T. D. W. 2016c. Chapter 12 - Experimental Methods. *High-Resolution NMR Techniques in*
550 *Organic Chemistry (Third Edition)*. Boston: Elsevier.
- 551 CUI, S. W. 2005. *Determination of Linkage Pattern: Methylation Analysis, Reductive Cleavage, and*
552 *Peroxidation* CRC Press.
- 553 D'AMELIO, N., PAPAMOKOS, G., DREYER, J., CARLONI, P. & NAVARINI, L. 2015. NMR studies of
554 hetero-association of caffeine with di-O-caffeoylquinic acid isomers in aqueous solution.
555 *Food Biophysics*, 10, 235-243.
- 556 DELLAROSA, N., TAPPI, S., RAGNI, L., LAGHI, L., ROCCULI, P. & DALLA ROSA, M. 2016. Metabolic
557 response of fresh-cut apples induced by pulsed electric fields. *Innovative Food Science &*
558 *Emerging Technologies*, 38, 356-364.
- 559 DING, H. H., CUI, S. W., GOFF, H. D., CHEN, J., WANG, Q. & HAN, N. F. 2015. Arabinan-rich
560 rhamnogalacturonan-I from flaxseed kernel cell wall. *Food Hydrocolloids*, 47, 158-167.
- 561 DU, X., ZHANG, Y., MU, H., LV, Z., YANG, Y. & ZHANG, J. 2015. Structural elucidation and antioxidant
562 activity of a novel polysaccharide (TAPB1) from *Tremella aurantialba*. *Food Hydrocolloids*,
563 43, 459-464.
- 564 EFIMOV, S. V., KHODOV, I. A., RATKOVA, E. L., KISELEV, M. G., BERGER, S. & KLOCHKOV, V. V. 2016.
565 Detailed NOESY/T-ROESY analysis as an effective method for eliminating spin diffusion from
566 2D NOE spectra of small flexible molecules. *Journal of Molecular Structure*, 1104, 63-69.
- 567 ELBANDY, M., RHO, J. R. & AFIFI, R. 2014. Analysis of saponins as bioactive zoochemicals from the
568 marine functional food sea cucumber *Bohadschia cousteaui*. *European Food Research and*
569 *Technology*, 238, 937-955.
- 570 ESATBEYOGLU, T., WRAY, V. & WINTERHALTER, P. 2013. Identification of two novel prodelphinidin
571 A-type dimers from roasted hazelnut skins (*Corylus avellana* L.). *Journal of Agricultural and*
572 *Food Chemistry*, 61, 12640-12645.
- 573 GE, Q., MAO, J.-W., ZHANG, A.-Q., WANG, Y.-J. & SUN, P.-L. 2013. Purification, chemical
574 characterization, and antioxidant activity of a polysaccharide from the fruiting bodies of
575 sanghuang mushroom (*Phellinus baumii* Pilát). *Food Science and Biotechnology*, 22, 301-
576 307.
- 577 GIL, R. R. & NAVARRO-VAZQUEZ, A. 2017. Chapter 1 Application of the Nuclear Overhauser Effect to
578 the Structural Elucidation of Natural Products. *Modern NMR Approaches to the Structure*
579 *Elucidation of Natural Products: Volume 2: Data Acquisition and Applications to Compound*
580 *Classes*. The Royal Society of Chemistry.
- 581 GONG, L., LI, T., CHEN, F., DUAN, X., YUAN, Y., ZHANG, D. & JIANG, Y. 2016. An inclusion complex of
582 eugenol into β -cyclodextrin: Preparation, and physicochemical and antifungal
583 characterization. *Food Chemistry*, 196, 324-330.
- 584 GUO, Q., CUI, S. W., KANG, J., DING, H., WANG, Q. & WANG, C. 2015. Non-starch polysaccharides
585 from American ginseng: physicochemical investigation and structural characterization. *Food*
586 *Hydrocolloids*, 44, 320-327.
- 587 HAYASHI, S., NAKANO, K. & YANASE, E. 2018. Investigation of color-deepening phenomenon in
588 catechin-(4 \rightarrow 8)-dimer as a proanthocyanidin model and structural determination of its
589 derivatives by oxidation. *Food Chemistry*, 239, 1126-1133.
- 590 HONG, S., WU, S., CAI, H., WANG, Y. & LIU, S. 2017. Instant structure profiling of substituted
591 catechins by chemical shift fingerprint of hydrogens of phenolic hydroxyl groups. *Journal of*
592 *Functional Foods*, 37, 58-65.
- 593 HU, T., HUANG, Q., WONG, K., YANG, H., GAN, J. & LI, Y. 2017. A hyperbranched β -d-glucan with
594 compact coil conformation from *Lignosus rhinocerotis sclerotia*. *Food Chemistry*, 225, 267-
595 275.
- 596 JAHED, V., ZARRABI, A., BORDBAR, A.-K. & HAFEZI, M. S. 2014. NMR (^1H , ROESY) spectroscopic and
597 molecular modelling investigations of supramolecular complex of β -cyclodextrin and

- 598 curcumin. *Food Chemistry*, 165, 241-246.
- 599 JIA, B.-X., ZENG, X.-L., REN, F.-X., JIA, L., CHEN, X.-Q., YANG, J., LIU, H.-M. & WANG, Q. 2014.
- 600 Baeckeins F-I, four novel C-methylated biflavonoids from the roots of *Baeckea frutescens*
- 601 and their anti-inflammatory activities. *Food Chemistry*, 155, 31-37.
- 602 JUNG, D.-M., DE ROPP, J. S. & EBELER, S. E. 2000. Study of interactions between food phenolics and
- 603 aromatic flavors using one- and two-dimensional ¹H NMR spectroscopy. *Journal of*
- 604 *Agricultural and Food Chemistry*, 48, 407-412.
- 605 KALIDAS, N. R., SAMINATHAN, M., ISMAIL, I. S., ABAS, F., MAITY, P., ISLAM, S. S., MANSHOOR, N. &
- 606 SHAARI, K. 2017. Structural characterization and evaluation of prebiotic activity of oil palm
- 607 kernel cake mannanoligosaccharides. *Food Chemistry*, 234, 348-355.
- 608 KEW, W., BELL, N. G. A., GOODALL, I. & UHRÍN, D. 2017. Advanced solvent signal suppression for the
- 609 acquisition of 1D and 2D NMR spectra of Scotch Whisky. *Magnetic Resonance in Chemistry*,
- 610 55, 785-796.
- 611 KFOURY, M., AUEZOVA, L., GREIGE-GERGES, H., RUELLAN, S. & FOURMENTIN, S. 2014. Cyclodextrin,
- 612 an efficient tool for trans-anethole encapsulation: Chromatographic, spectroscopic, thermal
- 613 and structural studies. *Food Chemistry*, 164, 454-461.
- 614 KIM, S.-D. 2013. α -Glucosidase inhibitor from *Buthus martensi* Karsch. *Food Chemistry*, 136, 297-
- 615 300.
- 616 KRINSKY, N. I. & JOHNSON, E. J. 2005. Carotenoid actions and their relation to health and disease.
- 617 *Molecular Aspects of Medicine*, 26, 459-516.
- 618 KUCHARSKA, A. Z., SZUMNY, A., SOKÓŁ-ŁĘTOWSKA, A., PIÓRECKI, N. & KLYMENKO, S. V. 2015.
- 619 Iridoids and anthocyanins in cornelian cherry (*Cornus mas* L.) cultivars. *Journal of Food*
- 620 *Composition and Analysis*, 40, 95-102.
- 621 KUMAR, A. & RANI GRACE, R. C. 2017. Nuclear Overhauser Effect A2 - Lindon, John C. In: TRANTER,
- 622 G. E. & KOPPENAAL, D. W. (eds.) *Encyclopedia of Spectroscopy and Spectrometry (Third*
- 623 *Edition)*. Oxford: Academic Press.
- 624 KUMOSINSKI, T. F., BROWN, E. M. & FARRELL, H. M. 1991. Molecular modeling in food research:
- 625 technology and techniques. *Trends in Food Science & Technology*, 2, 110-115.
- 626 LAU, B. F. & ABDULLAH, N. 2017. Bioprospecting of *Lentinus squarrosulus* Mont., an underutilized
- 627 wild edible mushroom, as a potential source of functional ingredients: A review. *Trends in*
- 628 *Food Science & Technology*, 61, 116-131.
- 629 LAVOINE, N., GIVORD, C., TABARY, N., DESLOGES, I., MARTEL, B. & BRAS, J. 2014. Elaboration of a
- 630 new antibacterial bio-nano-material for food-packaging by synergistic action of cyclodextrin
- 631 and microfibrillated cellulose. *Innovative Food Science & Emerging Technologies*, 26, 330-
- 632 340.
- 633 LE ROY, C. I., ŠTŠEPETOVA, J., SEPP, E., SONGISEPP, E., CLAUS, S. P. & MIKELSAAR, M. 2015. New
- 634 insights into the impact of *Lactobacillus* population on host-bacteria metabolic interplay.
- 635 *Oncotarget*, 6, 30545-30556.
- 636 LEE, S., LEE, D., LEE, S. O., RYU, J.-Y., CHOI, S.-Z., KANG, K. S. & KIM, K. H. 2017. Anti-inflammatory
- 637 activity of the sclerotia of edible fungus, *Poria cocos* Wolf and their active lanostane
- 638 triterpenoids. *Journal of Functional Foods*, 32, 27-36.
- 639 LÉVÈQUES, A., ACTIS-GORETTA, L., REIN, M. J., WILLIAMSON, G., DIONISI, F. & GIUFFRIDA, F. 2012.
- 640 UPLC-MS/MS quantification of total hesperetin and hesperetin enantiomers in biological
- 641 matrices. *Journal of Pharmaceutical and Biomedical Analysis*, 57, 1-6.
- 642 LI, Q., CAO, J., YUAN, W., LI, M., YANG, L., SUN, Y., WANG, X. & ZHAO, Y. 2017. New triterpene
- 643 saponins from flowers of *Impatiens balsamina* L. and their anti-hepatic fibrosis activity.
- 644 *Journal of Functional Foods*, 33, 188-193.
- 645 MARCO-RIUS, I., BOHNDIEK, S. E., KETTUNEN, M. I., LARKIN, T. J., BASHARAT, M., SEELEY, C. &
- 646 BRINDLE, K. M. 2014. Quantitation of a spin polarization-induced nuclear Overhauser effect
- 647 (SPINOE) between a hyperpolarized ¹³C-labeled cell metabolite and water protons.
- 648 *Contrast Media & Molecular Imaging*, 9, 182-186.

- 649 MASULLO, M., CERULLI, A., MARI, A., DE SOUZA SANTOS, C. C., PIZZA, C. & PIACENTE, S. 2017. LC-
650 MS profiling highlights hazelnut (Nocciola di Giffoni PGI) shells as a byproduct rich in
651 antioxidant phenolics. *Food Research International*, 101, 180-187.
- 652 MATENCIO, A., GARCÍA-CARMONA, F. & LÓPEZ-NICOLÁS, J. M. 2017. The inclusion complex of
653 oxyresveratrol in modified cyclodextrins: A thermodynamic, structural, physicochemical,
654 fluorescent and computational study. *Food Chemistry*, 232, 177-184.
- 655 MATYSIK, S., LE ROY, C. I., LIEBISCH, G. & CLAUS, S. P. 2016. Metabolomics of fecal samples: A
656 practical consideration. *Trends in Food Science & Technology*, 57, 244-255.
- 657 MÉNARD, O., BOURLIEU, C., DE OLIVEIRA, S. C., DELLAROSA, N., LAGHI, L., CARRIÈRE, F., CAPOZZI, F.,
658 DUPONT, D. & DEGLAIRE, A. 2018. A first step towards a consensus static in vitro model for
659 simulating full-term infant digestion. *Food Chemistry*, 240, 338-345.
- 660 MIRANDA-MOLINA, A., CASTILLO, E. & LOPEZ MUNGUÍA, A. 2017. A novel two-step enzymatic
661 synthesis of blastose, a β -d-fructofuranosyl-(2 \leftrightarrow 6)-d-glucopyranose sucrose analogue.
662 *Food Chemistry*, 227, 202-210.
- 663 PANTOJA PULIDO, K. D., COLMENARES DULCEY, A. J. & ISAZA MARTÍNEZ, J. H. 2017. New caffeic
664 acid derivative from *Tithonia diversifolia* (Hemsl.) A. Gray butanolic extract and its
665 antioxidant activity. *Food and Chemical Toxicology*, 109, 1079-1085.
- 666 PÉREZ GUTIÉRREZ, R. M. 2016. Anti-inflammatory effect of birsonimadiol from seeds of *Byrsonima*
667 *crassifolia*. *Food Science and Biotechnology*, 25, 561-566.
- 668 POVEDA, A. & JIMENEZ-BARBERO, J. 1998. NMR studies of carbohydrate-protein interactions in
669 solution. *Chemical Society Reviews*, 27, 133-144.
- 670 RADULOVIĆ, N. S., TODOROVSKA, M. M., ZLATKOVIĆ, D. B., STOJANOVIĆ, N. M. & RANDJELOVIĆ, P.
671 J. 2017. Two goitrogenic 1,3-oxazolidine-2-thione derivatives from Brassicales taxa:
672 Challenging identification, occurrence and immunomodulatory effects. *Food and Chemical*
673 *Toxicology*, 110, 94-108.
- 674 REIN, M. J., RENOUF, M., CRUZ-HERNANDEZ, C., ACTIS-GORETTA, L., THAKKAR, S. K. & DA SILVA
675 PINTO, M. 2013. Bioavailability of bioactive food compounds: a challenging journey to
676 bioefficacy. *British journal of clinical pharmacology*, 75, 588-602.
- 677 ROSS, A., SCHLOTTERBECK, G., DIETERLE, F. & SENN, H. 2007. Chapter 3 - NMR Spectroscopy
678 Techniques for Application to Metabonomics. In: LINDON, J. C., NICHOLSON, J. K. &
679 HOLMES, E. (eds.) *The Handbook of Metabonomics and Metabolomics*. Amsterdam: Elsevier
680 Science B.V.
- 681 RULE, G. S. & HITCHENS, T. K. 2006. *Fundamentals of Protein NMR Spectroscopy*, Springer
682 Netherlands.
- 683 SANDSTRÖM, C. & KENNE, L. 2006. Hydroxy Protons in Structural Studies of Carbohydrates by NMR
684 Spectroscopy. *NMR Spectroscopy and Computer Modeling of Carbohydrates*. American
685 Chemical Society.
- 686 SEDAGHAT DOOST, A., DEVLIEGHERE, F., DIRCKX, A. & VAN DER MEEREN, P. 2018a. Fabrication of
687 *Origanum compactum* essential oil nanoemulsions stabilized using Quillaja Saponin
688 biosurfactant. *Journal of Food Processing and Preservation*, 42, e13668.
- 689 SEDAGHAT DOOST, A., DEWETTINCK, K., DEVLIEGHERE, F. & VAN DER MEEREN, P. 2018b. Influence
690 of non-ionic emulsifier type on the stability of cinnamaldehyde nanoemulsions: A
691 comparison of polysorbate 80 and hydrophobically modified inulin. *Food Chemistry*, 258,
692 237-244.
- 693 SEDAGHAT DOOST, A., MUHAMMAD, D. R. A., STEVENS, C. V., DEWETTINCK, K. & VAN DER
694 MEEREN, P. 2018c. Fabrication and characterization of quercetin loaded almond gum-
695 shellac nanoparticles prepared by antisolvent precipitation. *Food Hydrocolloids*, 83, 190-
696 201.
- 697 SEDAGHAT DOOST, A., NIKBAKHT NASRABADI, M., KASSOZI, V., DEWETTINCK, K., STEVENS, C. V. &
698 VAN DER MEEREN, P. 2019. Pickering stabilization of thymol through green emulsification
699 using soluble fraction of almond gum – Whey protein isolate nano-complexes. *Food*

- 700 *Hydrocolloids*, 88, 218-227.
- 701 SEDAGHAT DOOST, A., SINNAEVE, D., DE NEVE, L. & VAN DER MEEREN, P. 2017. Influence of non-
702 ionic surfactant type on the salt sensitivity of oregano oil-in-water emulsions. *Colloids and*
703 *Surfaces A: Physicochemical and Engineering Aspects*, 525, 38-48.
- 704 SETTACHAIMONGKON, S., NOUT, M. J. R., ANTUNES FERNANDES, E. C., HETTINGA, K. A., VERVOORT,
705 J. M., VAN HOOIJDONK, T. C. M., ZWIETERING, M. H., SMID, E. J. & VAN VALENBERG, H. J. F.
706 2014. Influence of different proteolytic strains of *Streptococcus thermophilus* in co-culture
707 with *Lactobacillus delbrueckii* subsp. *bulgaricus* on the metabolite profile of set-yoghurt.
708 *International Journal of Food Microbiology*, 177, 29-36.
- 709 SHI, X.-D., NIE, S.-P., YIN, J.-Y., QUE, Z.-Q., ZHANG, L.-J. & HUANG, X.-J. 2017. Polysaccharide from
710 leaf skin of *Aloe barbadensis* Miller: Part I. Extraction, fractionation, physicochemical
711 properties and structural characterization. *Food Hydrocolloids*, 73, 176-183.
- 712 SPYROS, A. & DAIS, P. 2012. NMR Spectroscopy in Food Analysis. *Royal Society of Chemistry*, P001-
713 329.
- 714 TABORGA, L., SORTINO, M., CARRASCO, H., BUTASSI, E., ZACCHINO, S. & ESPINOZA, L. 2017.
715 Antifungal toxicity of linear geranylphenol. Influence of oxigenate substituents. *Food and*
716 *Chemical Toxicology*, 109, 827-835.
- 717 TEIXEIRA, N., MATEUS, N. & DE FREITAS, V. 2016. Updating the research on prodelphinidins from
718 dietary sources. *Food Research International*, 85, 170-181.
- 719 VÖGELI, B. 2014. The nuclear Overhauser effect from a quantitative perspective. *Progress in*
720 *Nuclear Magnetic Resonance Spectroscopy*, 78, 1-46.
- 721 WANG, J., NIE, S., CHEN, S., PHILLIPS, A. O., PHILLIPS, G. O., LI, Y., XIE, M. & CUI, S. W. 2017.
722 Structural characterization of an α -1, 6-linked galactomannan from natural *Cordyceps*
723 *sinensis*. *Food Hydrocolloids*, 78, 77-91.
- 724 WANG, S., JIN, D.-Q., XIE, C., WANG, H., WANG, M., XU, J. & GUO, Y. 2013. Isolation,
725 characterization, and neuroprotective activities of sesquiterpenes from *Petasites japonicus*.
726 *Food Chemistry*, 141, 2075-2082.
- 727 WILLIAMSON, M. P. 2009. Chapter 3 Applications of the NOE in Molecular Biology. *Annual Reports*
728 *on NMR Spectroscopy*. Academic Press.
- 729 WINNING, H., VIERECK, N., NØRGAARD, L., LARSEN, J. & ENGELSEN, S. B. 2007. Quantification of the
730 degree of blockiness in pectins using ¹H NMR spectroscopy and chemometrics. *Food*
731 *Hydrocolloids*, 21, 256-266.
- 732 XU, J., JI, F., CAO, X., MA, J., OHIZUMI, Y., LEE, D. & GUO, Y. 2016. Sesquiterpenoids from an edible
733 plant *Petasites japonicus* and their promoting effects on neurite outgrowth. *Journal of*
734 *Functional Foods*, 22, 291-299.
- 735 XU, X., XIE, H. & WEI, X. 2014. Jasmonoid glucosides, sesquiterpenes and coumarins from the fruit
736 of *Clausena lansium*. *LWT - Food Science and Technology*, 59, 65-69.
- 737 YIN, J.-Y., WANG, J.-Q., LIN, H.-X., XIE, M.-Y. & NIE, S.-P. 2016. Fractionation, physicochemical
738 properties and structural features of non-arabinoxylan polysaccharide from the seeds of
739 *Plantago asiatica* L. *Food Hydrocolloids*, 55, 128-135.
- 740 ZERAIK, M. L., QUEIROZ, E. F., MARCOURT, L., CICLET, O., CASTRO-GAMBOA, I., SILVA, D. H. S.,
741 CUENDET, M., DA SILVA BOLZANI, V. & WOLFENDER, J.-L. 2016. Antioxidants, quinone
742 reductase inducers and acetylcholinesterase inhibitors from *Spondias tuberosa* fruits.
743 *Journal of Functional Foods*, 21, 396-405.
- 744 ZHANG, A.-Q., LIU, Y., XIAO, N.-N., ZHANG, Y. & SUN, P.-L. 2014a. Structural investigation of a novel
745 heteropolysaccharide from the fruiting bodies of *Boletus edulis*. *Food Chemistry*, 146, 334-
746 338.
- 747 ZHANG, L.-J., LIAW, C.-C., HSIAO, P.-C., HUANG, H.-C., LIN, M.-J., LIN, Z.-H., HSU, F.-L. & KUO, Y.-H.
748 2014b. Cucurbitane-type glycosides from the fruits of *Momordica charantia* and their
749 hypoglycaemic and cytotoxic activities. *Journal of Functional Foods*, 6, 564-574.
- 750

Highlights

- Principle and applications of nuclear and rotating-frame Overhauser effects.
- Characterization of stereochemical structure using the NMR techniques.
- The complex inclusion of novel compounds could be investigated.